博士論文

New Crystalline Porous Materials with Photophysical and Photochemical Functions

（光物理・光化学的機能を有する新規結晶性多孔質材料）

黄 虎彪

[1] Introduction

Crystalline porous solids are of particular scientific and technological importance due to their ability to interact with atoms, ions, and molecules at both the surfaces and throughout the bulk of the interior of the materials. Since the first discovery of the natural porous crystalline zeolite, stilbite, in 1756, there have been significant advances in the ability to fabricate new porous solids with ordered structures from a wide range of materials by synthetic chemistry. Among them, two preventatives are porous silica and zeolites. These two classes of crystalline porous materials show a wide range of applications for traditional use as catalysts and adsorbents.[1] However, to meet the requirements for more advanced applications, such as fuel storage, sensors, drug delivery, and optoelectronics, there has been an increasing need to engineer greater uniformity in pore size, geometry and pore surface at the molecular level. In this regard, one of the most important sub-disciplines of supramolecular chemistry, metal-organic frameworks (MOFs), stands out as optimal materials to address these issues. MOFs are constructed by the coordination of transition metal ions (Zn^{2+}, Cu^{2+}, Cd^{2+}, Eu^{3+}, Zr^{4+}, etc.) and di-/polytopic organic linkers.[2] They possess permanent porosity, well-defined pore structures, and tailored pore surfaces (Figure 1). More importantly, this class of crystalline porous solids enables chemists and materials scientists to tailor the functionalities of the pore space in the MOFs by the rational design of building blocks at a molecular level for specific recognitions toward various ions, gaseous molecules, or even small drugs, which extends the applications of MOFs to more sophisticated systems, as mentioned above. The manipulation of the MOFs' functionality via remote and noninvasive methods through the incorporation of light-responsive building blocks is a promising area of research.[3] Inspired by the previous works in photo-responsive porous crystalline solids, the research projects I have worked on in my three years of Ph. D. studies mainly emphasized the design and synthesis of novel crystalline porous materials featuring unique photophysical and photochemical functionality.

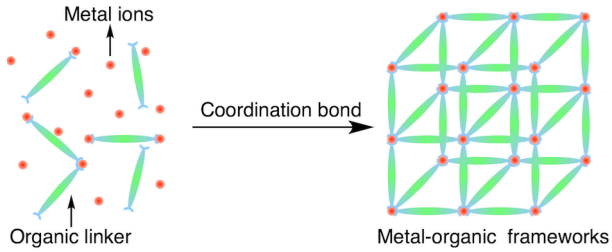

Figure 1. A scheme of assembly of metal-organic frameworks by coordiantion of transition metal ions and organic linkers.

[2] Crystalline Nanochannels with Pendant Azobenzene Groups

The integration of photoresponsive functional groups, such as azobenzenes, diarylethenes, aryl azides, and nitrobenzyl moieties, into MOFs is a leading strategy for realizing remote and noninvasive manipulation of their properties. Azobenzene derivatives are well-known photoswitches that provide large geometrical changes based on their photochemical isomerization upon irradiation with ultraviolet (UV) and visible light. This isomerization also provides a remarkable change in polarity because the

dipole moments of the *trans*- and *cis*-isomers of non-substituted azobenzene are approximately zero and 3.1 D, respectively. While azobenzene moieties have previously been incorporated into crystalline porous solids, to the best of my knowledge, no claim was given as to how the change in polarity of the pore surfaces upon the *cis*-/*trans*- isomerization affects the diffusion kinetics of gaseous molecules through MOFs. Herein, we report on the synthesis of a zirconium-based metal-organic framework with pendant azobenzene groups (^{Azo}MOF, $Zr_6O_4(OH)_4L_6$; L^{2-} = 2'-phenyldiazenyl-1,1':4',1''-terphenyl-4,4''-dicarboxylate, Figure 2a). Single crystals (Figures 2b inset) suitable for X-ray diffraction analysis were obtained, along with powdery crystalline samples used for spectroscopic studies (Figures 2b). The obtained crystal structure revealed that ^{Azo}MOF consists of small tetrahedral and large octahedral pores (Figure 2c), which are connected heterotropically through shared triangular windows (Figure 2d). Upon irradiation with ultraviolet (UV) light at 365 ± 10 nm, ^{Azo}MOF underwent a 21% conversion of *trans*-to-*cis* isomerization of its pendant azobenzene moieties

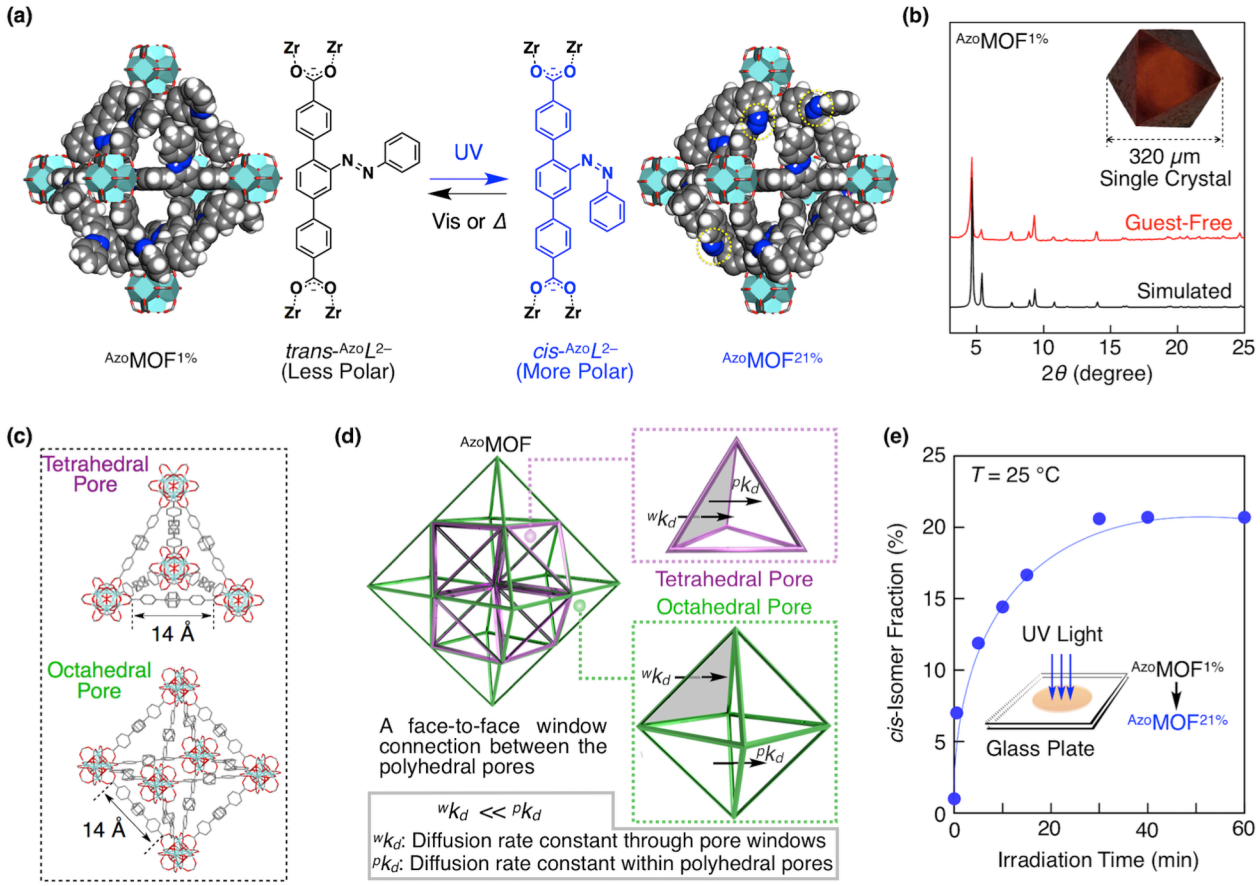

Figure 2. **(a)** A schematic representation of ^{Azo}MOF with azobenzene (Azo) groups as photo-isomerizable pendants. The Azo groups adopting a *cis* configuration are highlighted with yellow circles. **(b)** Powder X-ray diffraction (PXRD) pattern of guest-free ^{Azo}MOF (red) and a simulated pattern for as-synthesized ^{Azo}MOF (black). The inset in **(b)** shows an optical image of a single crystal of ^{Azo}MOF$^{1\%}$. **(c)** Single-crystal structures of tetrahedral and octahedral pores in ^{Azo}MOF. **(d)** A schematic illustration of the pore structures in ^{Azo}MOF. The tetrahedral and octahedral pores are highlighted in purple and green colors, respectively. **(e)** ^{1}H NMR evaluation of the *trans*-to-*cis* isomerization in ^{Azo}MOF upon irradiation with UV light (365 ± 10 nm) at 25 °C.

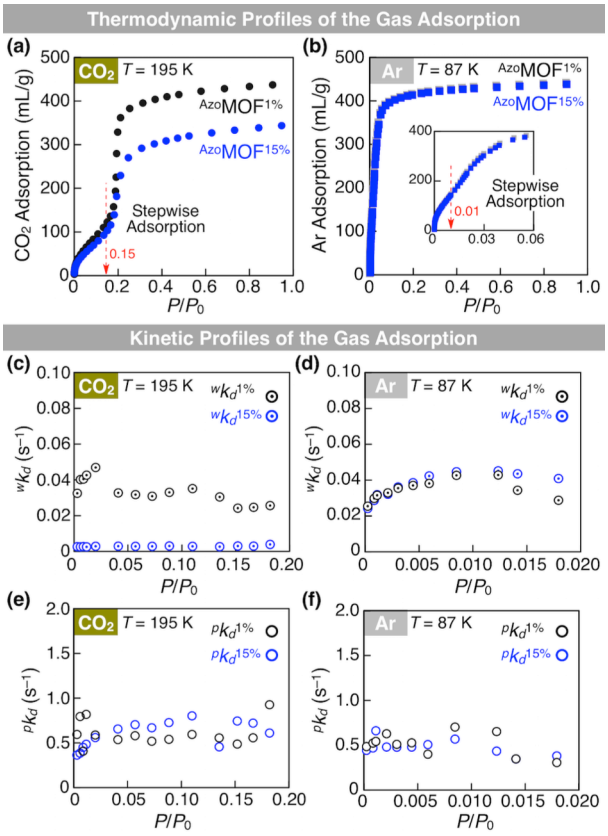

Figure 3. Adsorption isotherms of **(a)** CO_2 at 195 K and **(b)** Ar at 87 K in $^{Azo}MOF^{1\%}$ (black) and $^{Azo}MOF^{15\%}$ (blue), respectively, where the inflection points for the secondary adsorption to start appear at P/P_0 = 0.15 and 0.01, respectively. The inset in **(b)** shows adsorption isotherms of Ar enlarged in a range of P/P_0 from 0 to 0.06. Diffusion rate constants for **(c)** CO_2 (P/P_0 = 0–0.2) and **(d)** Ar (P/P_0 = 0–0.02) through the triangular windows ($^{w}k_d$) in $^{Azo}MOF^{1\%}$ (black) and $^{Azo}MOF^{15\%}$ (blue), respectively. Diffusion rate constants for **(e)** CO_2 (P/P_0 = 0–0.2) and (f) Ar (P/P_0 = 0–0.02) within the polyhedral pores ($^{p}k_d$) in $^{Azo}MOF^{1\%}$ (black) and $^{Azo}MOF^{15\%}$ (blue), respectively.

($^{Azo}MOF^{21\%}$) in 30 min at the photostationary state (Figure 2e). The reverse process, isomerization from *cis*-to-*trans*, could be achieved upon either irradiation with visible light (420–480 nm) or heating. The isomerization exerts a significant effect on the adsorption of CO_2 but not on the adsorption of Ar in the ^{Azo}MOF (Figure 3a). These contrasting behaviors are quite interesting, as the kinetic diameters of CO_2 (3.4 Å) and Ar (3.3 Å) are nearly identical to one another. However, CO_2 has a quadrupole moment (-14.9×10^{-40} C m^2), although both CO_2 and Ar are apolar. In accord with this observation, the Brunauer–Emmet–Teller (BET) surface areas evaluated with Ar for $^{Azo}MOF^{1\%}$ (1412 m^2 g^{-1}) and $^{Azo}MOF^{15\%}$ (1418 m^2 g^{-1}) were essentially identical. Therefore, it is likely that the difference in adsorption isotherms between CO_2 and Ar is due to the CO_2 molecules experiencing an attractive effect from the dipole/quadrupole interactions rather than from a steric effect due to changes in the configuration of azobenzene groups. When erythrosine B, a polarity-sensitive agent, was used as the guest, it showed a red shift upon exposure of $^{Azo}MOF^{20\%}\supset$EB to visible light, indicating that the interior environment of ^{Azo}MOF becomes less polar as the *trans*-isomer content increases.

Fitting each kinetic profile of CO_2 and Ar using a double-exponential equation gave a sequence of values for the two diffusion rate constants,[4] $^{w}k_d$ and $^{p}k_d$, which are attributed to the diffusion rate constants of gaseous molecules through the triangular windows and within the polyhedral pores, respectively (Figure 2d). As expected, regardless of the *cis*-isomer content of ^{Azo}MOF, the $^{w}k_d$ values for both CO_2 (Figures 3c and 3e) and Ar (Figures 3d and 3f) are much smaller than the corresponding $^{p}k_d$ values over the whole range of P/P_0 (P = equilibrium vapor pressure, P_0 = saturated vapor pressure). Of particular interest is the fact that the $^{w}k_d$ values for CO_2 in $^{Azo}MOF^{15\%}$ (blue) are one-order of magnitude smaller than those in $^{Azo}MOF^{1\%}$ (black) (Figure 3c). In sharp contrast, the $^{p}k_d$ values for CO_2 in $^{Azo}MOF^{15\%}$

(blue) and ^{Azo}MOF$^{1\%}$ (black) are almost identical to one another (Figure 3e). Namely, the azobenzene *cis*-isomer content of ^{Azo}MOF mostly influences the diffusion events through the triangular windows. Meanwhile, as shown in Figures 3d and 3f, such a site-specific effect of the azobenzene isomer content on the diffusion process (black and blue) was not observed for Ar. Together with the facts that the kinetic diameters of CO_2 (3.4 Å) and Ar (3.3 Å) are essentially identical to one another and that the azobenzene pendants are localized on the window frames (Figure 3c), the marked difference in the $^{w}k_d$ values for CO_2 absorbed in ^{Azo}MOF$^{1\%}$ and ^{Azo}MOF$^{15\%}$ ($^{w}k_d$ in ^{Azo}MOF$^{1\%}$ >> $^{w}k_d$ in ^{Azo}MOF$^{15\%}$) suggests that the diffusion of CO_2 is affected by polarity effects, due to the large quadrupole moment, rather than from steric effects. One further aspect that requires clarification is why the amount of adsorbed CO_2 in ^{Azo}MOF$^{15\%}$ is smaller than that in ^{Azo}MOF$^{1\%}$. The physical properties of CO_2 in the condensed state, including quadrupole/quadrupole interactions, could be affected by the coexistence of polar groups in the congested space. In fact, surface groups in such crystalline nanochannels have been reported to influence the packing modes of gaseous molecules condensed within. We suppose that this is also the case in the crystalline nanochannels of ^{Azo}MOF, where the packing mode, and thus the density of CO_2 would change with the polarity of the channel wall, i.e., the *cis*-isomer content of the azobenzene pendants.

In conclusion, we demonstrated that ^{Azo}MOF provides the first porous crystalline nanochannel to photochemically modulate the diffusion kinetics of CO_2 by alteration of the dipole/quadrupole interactions within the azobenzene-appended channel wall.

[3] Self-Assembled Porphyrin-Based Crystalline Microstructure

Nano- or microstructures constructed from electrically and optically active organic molecules display unusual optoelectronic properties, often quite different with respect to the single molecules or the bulk materials. Porphyrins (**Por**) are versatile functional molecules in catalysis, light harvesting and molecular sensing. They are particularly attractive building blocks for self-assembled nano- or microstructures because of its square-planar nature and unique photophysical and photochemical properties. Several unique **Por**-based nanostructures, such as nanofibers, nanotubes and nanosheets, have been fabricated *via* supramolecular assembly. These assemblies have shown intriguing optoelectronic or catalytic properties.

Herein, we report a serendipitous discovery that a new porphyrin-based crystalline microstructure was obtained from a reaction mixture of *meso*-tetra(4-carboxyphenyl)porphine (^{2H}**Por**), 4,4'-azopyridine (^{Azo}**Py**) and $Zn(NO_3)_2$ in a mixture of DMF/EtOH (*v*/*v* = 3:1) via a solvothermal reaction (Figure 4a). This crystalline microstructure possessed a peripheral square crystal and a cubic crystal centered on the corresponding peripheral crystal. It was found that the concentration of reaction mixture as well as the reaction time played a key role for the nucleation and crystal growth of such crystalline microstructures.

^{1}H NMR and diffusion reflectance spectroscopy analyses revealed that the peripheral square crystal was consisting of zinc porphyrin (**^{Zn}Por**) only, while the cubic crystal was composed of **^{Zn}Por** and **^{Azo}Py** with a molar ratio of one to one. Scanning electron microscopy (SEM) and atomic force microscopy (AFM) observations revealed that a layer-by-layer structure was observed in both the peripheral and the cubic crystals. Selective area electron diffraction (SAED) analyses showed that they possessed a good single crystallinity. By combining the SAED and grazing incident X-ray diffraction analyses, the basic layered structure in both the peripheral and the cubic crystals was the two-dimensional networks of zinc-metalated porphyrins connected by paddle-wheel-like zinc–carboxylate clusters. It is noteworthy that the cubic crystal could be isolated from the crystalline microstructure (Figure 4a); and the attained cubic crystal exhibited a dichroism phenomenon under linearly polarized light (Figures 4b-4d), suggesting a layered stacking of porphyrin networks in the cubic crystal, which was consistent with the observations by SEM and AFM. When an intact porphyrin-based crystalline microstructure was placed under the confocal laser scanning microscopy (CLSM) with an excitation (Ex.) laser of 488 nm, it exhibited unique photoluminescence properties (Figures 4e and 4f), where the peripheral crystal showed a bright fluorescence emission but negligible fluorescence emission was observed from the corresponding cubic crystal. When the core was isolated from the corresponding crystalline microstructure, the hollow peripheral crystal still retained strong fluorescence emission (Figure 4g). Surprisingly, a fluorescence emission was observed in the cubic crystal under

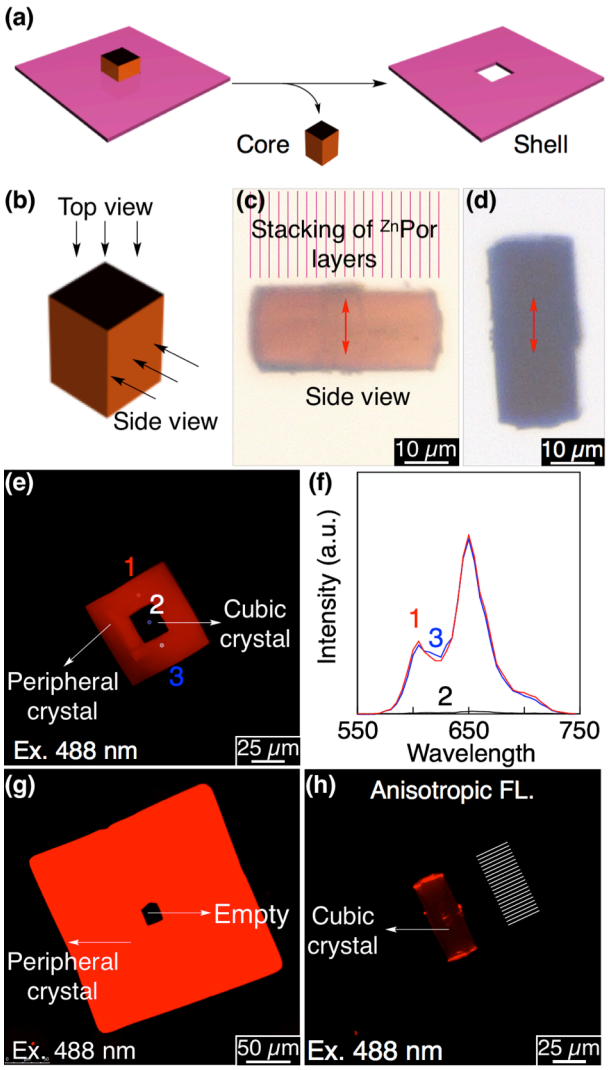

Figure 4. **(a)** A schematic illustration of separating the cubic crystal from the intact porphyrin-based crystalline microstructure. **(b)** The view direction of the cubic crystal by linearly polarized light. **(c)** and **(d)** represent side-view pictures under linearly polarized light. The inset in **(c)** show a stacking mode of 2D **^{Zn}Por** layers. **(e)** An observation of an intact porphyrin-based crystalline microstructure by CLSM with an excitation wavelength of 488 nm; and **(f)** the fluorescence intensity of the corresponding porphyrin-based crystalline microstructure. Observations of **(g)** a hollow peripheral crystal and **(h)** a cubic crystal under CLSM with an excitation wavelength of 488 nm.

CLSM (Figure 4h), in sharp contrast to the case in the intact porphyrin-based crystalline microstructure (Figure 4e). We assume that this anisotropic fluorescence in the cubic crystal might be due to wave-guiding phenomenon in the cavities of core crystal.

In summary, we synthesized a novel porphyrin-based crystalline microstructure with intriguing photophysical properties. The structures and compositions of this porphyrin-based crystalline microstructure were investigated by SEM, TEM, PXRD and ^{1}H NMR spectroscopic analyses.

[4] Conclusion

My research projects emphasize the synthesis and properties of azobenzene-functionalized metal-organic frameworks and porphyrin-based crystalline microstructure. Both of them exhibit unprecedented photophysical and photochemical properties. What I have achieved in my research projects is an important and insightful complement to the fundamental photochemistry of crystalline porous materials.

[5] References

(1) M. E. Davis. *Nature.* **2002**, *417*, 813.

(2) H. Furukawa, K.E. Cordova, M. O'Keffe, O. M. Yaghi, *Science*, **2013**, *341*, 974.

(3) Sato, H.; Matsuda, R.; Sugimoto, K.; Takata, M.; Kitagawa, S. *Nat. Mater.* **2010**, *9*, 661.

(4) Choi, H. J.; Dinca, M.; Long, J. R. *J. Am. Chem. Soc.* **2008**, *130*, 7848.

[6] Publications

[1] H. B. Huang, H. Sato, T. Aida. Crystalline nanochannels with pendant azobenzene groups: steric or polar effects on gas adsorption and diffusion, *J. Am. Chem. Soc.* **2017**, *139*, 8784–8787.

[2] H. B. Huang, H. Sato, T. Aida. A novel porphyrin-based crystalline microstructure featuring unprecedented optical properties, *to be submitted***.**